J. Astrophys. Astr. (2010) **31,** 105–119

Extracting Information from the Gravitational Redshift of Compact Rotating Objects

Paul D. Nuñez[*,†] & Marek Nowakowski[**]
[*]*Department of Physics & Astronomy, University of Utah, 115 S 1400 E, Salt Lake City, UT 84112* and *Observatorio Astronómico, Universidad Sergio Arboleda, Cll. 74 No. 14–14, Bogotá, Colombia.*
[**]*Departamento de Física, Universidad de los Andes, Cra. 1E No. 18A-10, Bogotá, Colombia.*
[†]*email: nunez.paul@gmail.com*

Received 2010 February 16; accepted 2010 May 4

Abstract. Essential macroscopic internal properties of compact objects can be related to each other with the help of General Relativity. A somewhat familiar example is the relationship between the compactness M/R and the gravitational redshift for nonrotating bodies. Rotation poses new challenges when trying to relate observed or potentially observed quantities such as the graviational redshift, mass, radius, and angular velocity. Using a perturbative approach, we present an analytical approximation whose purpose is to relate these quantities. Two main results are highlighted: Derivation of a new maximal angular velocity depending only on the mass of the object and a possible estimate of the radius from a measurement of the gravitational redshift.

Key words. Maximal angular velocity—stars: neutron—stars: rotation.

1. Introduction

Compact objects such as neutron stars[1] have radii very close to their Schwarzschild radii (Friedman 1995) and hence General Relativity should be used to describe the gravity close to their surface. Neglecting rotation, the geometry of space-time can be described using the well known spherically symmetric Schwarzschild geometry and information on the ratio M/R of a compact object can be obtained from the (observed) gravitational redshift (Becker & Pavlov 2002; Pavlov & Zavlin 2003). This is a useful, model-independent way, to gain insight into properties of neutron stars and white dwarfs. Although it is a model-independent procedure, it relies on certain basic assumptions like the absence of rotation and a perfect spherical symmetry (i.e., zero quadrupole moment). To gain a deeper understanding it makes sense to relax some of these assumptions and to examine what information can be extracted from the gravitational redshift in the more general case. In the present paper, we shall study the situation with a non-zero angular velocity Ω, but assuming that the object is rigid enough to allow the approximation of a negligible quadrupole moment. In particular,

[1]For a review, see Stergioulas (2003).

when rotation is taken into account, spherical symmetry is lost and off diagonal terms appear in the metric which has the following general form:

$$ds^2 = g_{tt}dt^2 + g_{rr}dr^2 + g_{\theta\theta}d\theta^2 + g_{\phi\phi}d\phi^2 + 2g_{\phi t}d\phi dt. \quad (1)$$

The exact form of this metric including magnetic field, quadrupole moment and even radiation (Vadya 1951) is still a subject of research (Manko *et al.* 2000; Pachon *et al.* 2006). We will use a first and second order approximation to this metric neglecting the effects of the quadrupole moment and the magnetic field. Furthermore, it is expected that only relatively young neutron stars can have a differential rotation (Stergioulas 2003) (encountered also in boson stars (Schunck & Mielke 2003)) which we therefore neglect here. It is therefore of some importance to specify clearly the goals of the paper. In Friedman *et al.* (1986) an exhaustive numerical investigation of rotating neutron stars has been performed relying on the choice of the equation of state in the interior. We in contrast do not aim at precision here, but rather at short analytical results which can give us the correct order of magnitude and physical insight. In doing so we also maintain, as far as this is possible, a certain model independence whereby model we mean some input which requires knowledge of the interior of the star.

Deriving the gravitational redshift from equation (1) we will show that, for a fixed mass, a unique solution for the radius of the compact object does not exist. Instead, we obtain two different solutions which can differ by orders of magnitude as long as the angular velocity is not too large. In this case, all theoretical models still favour the solution of the smaller radius and we can select this solution without the necessity to refer to some details of a specific model. With increasing angular momentum, the two radii approach each other and the above selection rule is not effective anymore. However, in such a case we can define a narrow range of allowed radii which is still a valuable model independent information for fast rotating objects.

Another main result derived from our examination of the properties of the gravitational redshift $\mathcal{Z}$, is that there exists an upper bound on the angular velocity depending on the redshift. One can even put an absolute upper bound which is independent of $\mathcal{Z}$. Interestingly the bounds come out to be in the range of the observed millisecond pulsars and comparable to the results obtained by numerical simulations performed by Salgado *et al.* (1994a, 1994b). This in turn allows us to assume that the angular velocity of millisecond pulsars is indeed approaching its maximal value. The consequences of this assumption will be discussed in the text below. One of them is the confirmation of the result that the light emitted in very fast millisecond pulsars stems mostly from the equatorial region (Kuzmin & Wu 1992; Backer 1998; Chen *et al.* 1998). We compare our results to the so called 'Mass Shedding Limit' (Lattimer *et al.* 1990) and to other works related to the maximum angular velocity.

The essential parameters which enter our equations are the radius R, the angular velocity Ω and the mass M. The minimum central density at which a neutron star is stable is simply the density at which neutrons become unstable to beta decay ($\rho_0 \approx 8 \times 10^6$ g/cm^3 (Baym & Lamb 2005)). Using the well known Oppenheimer–Volkov (Oppenheimer & Volkov 1939) equations and a plausible equation of state, one can construct a stellar model which provides the minimum mass of the neutron star to be around $0.08\,\mathrm{M}_\odot$ which is a bit unrealistic taking into account that neutron stars are remnants of supernova explosions (Baade & Zwicky 1934). A more realistic value for the minimum mass is of the order of $M_{\mathrm{NS}}^{\mathrm{min}} \approx 1\,\mathrm{M}_\odot$ (Lattimer & Prakash 2004), which is actually closer to the maximum mass of a white dwarf ($1.44\,\mathrm{M}_\odot$). The maximum

mass of a neutron star can be found from causality arguments (Rhoades & Ruffini 1974), by recalling that the speed of sound in dense matter has to be less than the speed of light ($dp/d\rho \leq c^2$). This condition gives a maximum mass of $M_{\rm NS}^{\rm max} \approx 3\,{\rm M}_\odot$. The radii corresponding to the maximum and minimum masses can be found using the Oppenheimer–Volkov equation. Assuming an equation of state for a degenerate neutron fluid, the corresponding radii for the two extreme masses lie in the range ~ 10 km to ~ 100 km. This radius range can of course change if one uses a more sophisticated equation of state, subject of current controversy (Lattimer & Praksah 2004), but the orders of magnitude remain the same (Shapiro & Teukolsky 1983). The canonical neutron star mass and radius are thought to be $\sim 1\,{\rm M}_\odot$ and ~ 10 km. A useful observational quantity, which agrees in order of magnitude with theoretical predictions, is the mean 'measured' mass of the neutron stars in a Gaussian ensemble (Thorsett & Chakrabarty 1999), namely:

$$\langle M \rangle_{\rm NS} = (1.35 \pm 0.05){\rm M}_\odot. \tag{2}$$

This value will be used if no other information on the masses is available.

The paper is organized as follows. In the second section, we will briefly discuss the gravitational redshift as emerging from a perturbative axial symmetric metric. In section three, we will use these results to determine the radius or the range of the radii of the compact object. Section four is devoted to the maximal angular velocity derived within our approach. In section five, we discuss some improvements by taking into account more terms in the expansion of the metric. In section six, we apply our results to some chosen compact objects like a white dwarf and neutron stars. Finally, in section seven we present our conclusions.

2. The gravitational redshift in a perturbation approach

A far away observer can measure a pulsar's angular velocity Ω as:

$$\Omega = \frac{d\phi}{dt} = \frac{d\phi}{d\tau}\frac{d\tau}{dt} = \frac{u^\phi}{u^t}. \tag{3}$$

Using equation (3), the four velocity of a stationary point on the surface can be written as:

$$u^\mu = (u^t, 0, 0, \Omega u^t). \tag{4}$$

Through the normalization condition of the four velocity ($u_\mu u^\mu = -1$), we obtain the time-like component of the four velocity in terms of the metric (1) and angular velocity Ω:

$$u^t = (-g_{tt} - 2g_{t\phi}\Omega - \Omega^2 g_{\phi\phi})^{-1/2}. \tag{5}$$

The redshift factor can be calculated simply by recalling that the energy of a radial photon ($\hbar = c = 1$) is simply (Carroll 2004)

$$\begin{aligned}\omega &= u^\mu \frac{dx_\mu}{d\lambda} = u^t\left(g_{tt}\frac{dt}{d\lambda} + g_{t\phi}\frac{d\phi}{d\lambda}\right) + u^\phi\left(g_{\phi t}\frac{dt}{d\lambda} + g_{\phi\phi}\frac{d\phi}{d\lambda}\right)\\ &= u^t E + u^\phi L = u^t(E + \Omega L),\end{aligned} \tag{6}$$

with λ an affine parameter and E and L conserved quantities due to the existence of two killing vectors. As a consequence we can write ω as:

$$\omega = \frac{E + \Omega L}{(-g_{tt} - 2g_{t\phi}\Omega - \Omega^2 g_{\phi\phi})^{1/2}}, \tag{7}$$

and the energy perceived by a distant observer ω can be now expressed through

$$\omega = \mathcal{Z}\omega_0, \tag{8}$$

where ω_0 is the energy at the surface and $\mathcal{Z}$ is the redshift factor. Explicitly, the latter is given by:[2]

$$\mathcal{Z} = (-g_{tt} - 2g_{t\phi}\Omega - \Omega^2 g_{\phi\phi})^{1/2}. \tag{9}$$

This redshift can actually be measured for many objects.[3] Indeed, at the end of the paper we will employ the results of such observations. The behaviour of $\mathcal{Z}$ as a function of the radius R for a fixed mass is displayed in Fig. 1(a).

The calculation of $\mathcal{Z}$ can be made more concrete when we consider the metric (1). To a first approximation, Zeldovich and Novikov (Zeldovich & Novikov 1971) apply small perturbations to the Schwarzschild geometry. The elements of the metric (1) can be calculated as (Zeldovich & Novikov 1971):

$$g_{tt} = -\left(1 - \frac{2GM}{Rc^2}\right), \quad g_{t\phi} = \frac{2GJ\sin^2\theta}{Rc^4}, \quad g_{\phi\phi} = \frac{R^2\sin^2\theta}{c^2}. \tag{10}$$

Here the condition for slow rotation is given by $J \ll MR_g c$ (R_g being the Schwarzschild radius) (Zeldovich & Novikov 1971). This condition will always be satisfied and will be discussed at the end of section 4. In passing we note that Ω^2 terms in g_{tt} are, in principle, possible. We justify the neglecting of such terms *a posteriori*, i.e., by the successful prediction of the maximal angular velocity and of some radii. Equation (10) allows us to calculate $\mathcal{Z}$ explicitly. One obtains:

$$\mathcal{Z}(M, R, \Omega, J) = \left(1 - \frac{2GM}{c^2 R} - \frac{4GJ\Omega\sin^2\theta}{c^4 R} - \frac{R^2\Omega\sin^2\theta}{c^2}\right)^{1/2}. \tag{11}$$

Throughout the paper we will be using the Newtonian approximation for the angular momentum ($J = (2/5)MR^2\Omega$).[4] In view of the results obtained in Cook *et al.* (1994), this is a well-based assumption violated only for extremely high angular velocities (which are not exceeded here). Taking this into account, equation (11) simplifies to:

$$\mathcal{Z}(M, R, \Omega') = \left(1 - \alpha\frac{M}{R} - \beta MR\,\Omega'^2 - \gamma R^2\Omega'^2\right)^{1/2}, \tag{12}$$

[2]This redshift factor is often defined as $(1 + \mathcal{Z})^{-1}$ instead of just $\mathcal{Z}$. This expression was first obtained by Luminet (1979) in a different context.

[3]Even the gravitational redshift of the Sun has been measured (Snider 1972; Krisher *et al.* 1993).

[4]Angular momentum has a problem of factor 2 in General Relativity, see for instance, Wald (1984) and Mielke (2001) and references therein.

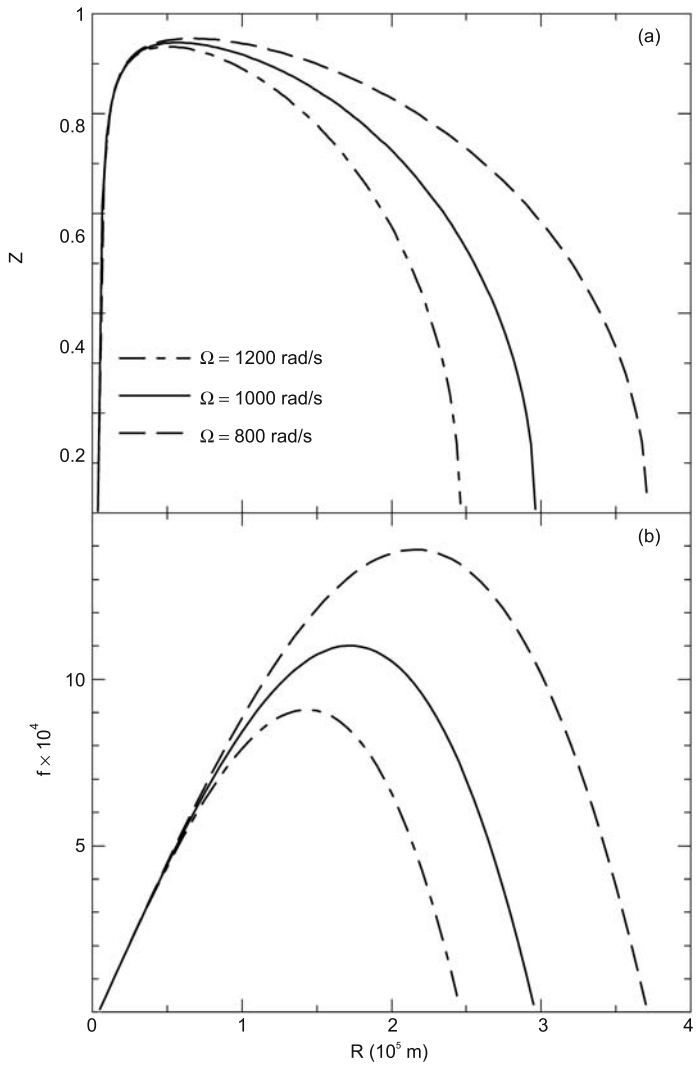

Figure 1. The top figure **(a)**, shows the behaviour of the redshift equation (12) as a function of the radius for different angular velocities. The bottom figure **(b)** shows the behaviour of the corresponding polynomial (15) in units of meters. In both figures $M = 1.44\,\mathrm{M}_{\odot}$. Note how the gap between the two solutions becomes narrow with increasing angular velocity.

where α, β and γ are constants given by:

$$\alpha = \frac{2G}{c^2}, \quad \beta = \frac{8G}{5c^4}, \quad \gamma = \frac{1}{c^2}, \tag{13}$$

and we have absorbed $\sin\theta$ into the angular momentum by defining

$$\Omega' \equiv \sin\theta\,\Omega. \tag{14}$$

The equations (9), (13) and (14) can be now used to either solve them for the radius by assuming a mean mass or a mass range and a measured angular velocity or, alternatively to predict the redshift. Both ways will be used below.

3. Determination of the radius

It is possible to take two different approaches when using equation (12). The first one is to demand that the term inside the parenthesis of equation (12) should be greater than zero, such that after factoring out $1/\sqrt{R}$ one arrives at:

$$f(0; R, M, \Omega) \equiv R - \alpha M - \beta M R^2 \Omega^2 - \gamma R^3 \Omega^2 \geq 0. \tag{15}$$

The limiting values of R correspond to the equal sign in the above equation. Since this does not depend on $\mathcal{Z}$, these values have an absolute character in the sense that they give the maximal and minimal radius for any compact object with mass M and angular velocity Ω regardless of the value of $\mathcal{Z}$. Similar reasoning applies to any other quantity derived from equation (15) (e.g., $\Omega'_{\max}$ in the next section).

The behaviour of the function $f(0; R, M, \Omega)$ *versus* R is shown in Fig. 1(b). The figure displays the global properties of this function (which can also be inferred easily analytically), like the local maximum and the two zeros, one of them close to the Schwarzschild radius.

On the other hand, we can solve the following cubic equation for the radii:

$$f(\mathcal{Z}; R, M, \Omega) = (1 - \mathcal{Z}^2)R - \alpha M - \beta M R^2 \Omega^2 - \gamma R^3 \Omega^2 = 0. \tag{16}$$

Obviously, this is the same equation as (15) if we put $\mathcal{Z}$ to zero in equation (16). Hence, we can continue examining equation (16) and discuss the absolute limits by putting $\mathcal{Z} = 0$ at the end. The function f with non-zero gravitational redshift has the same global properties as equation (15). The solutions of equation (16) can be obtained analytically by parameterizing the Cardano formulae (Bronstein & Semendjajew 2004). By a simple transformation one can get rid of the quadratic term in the cubic equation arriving at $y^3 + py + q = 0$. Depending on the sign of the discriminant $D = (p/3)^3 + (q/2)^2$, one can parametrize the solution using the auxiliary variable $\mathcal{F} = \mathrm{sgn}(q)\sqrt{|p|/3}$. In our case $D \geq 0$ and we parametrize the solutions through the angle α given by $\cos\alpha = q/e\mathcal{F}^3$. The analytical solutions are then:

$$r_1 = -\Delta - \mathcal{A}\cos\left\{\frac{2\pi}{3} + \frac{1}{3}\cos^{-1}\chi\right\}, \tag{17}$$

$$r_2 = -\Delta - \mathcal{A}\cos\left\{\frac{4\pi}{3} + \frac{1}{3}\cos^{-1}\chi\right\}, \tag{18}$$

where

$$\Delta \equiv \frac{M\beta}{3\gamma}, \qquad \mathcal{A} \equiv \frac{2}{3}\sqrt{\frac{M^2\beta^2}{\gamma^2} + \frac{3}{\gamma\Omega^2}} \tag{19}$$

and

$$\chi \equiv \frac{27\left\{\frac{1024}{3375}\left(\frac{GM\Omega}{c^3}\right)^3 + 2\frac{GM\Omega}{c^3} + \frac{8(1-\mathcal{Z}^2)}{15}\frac{GM\Omega}{c^3}\right\}}{2\left\{\frac{64}{25}\left(\frac{GM\Omega}{c^3}\right)^2 + 3(1-\mathcal{Z}^2)\right\}^{3/2}}. \tag{20}$$

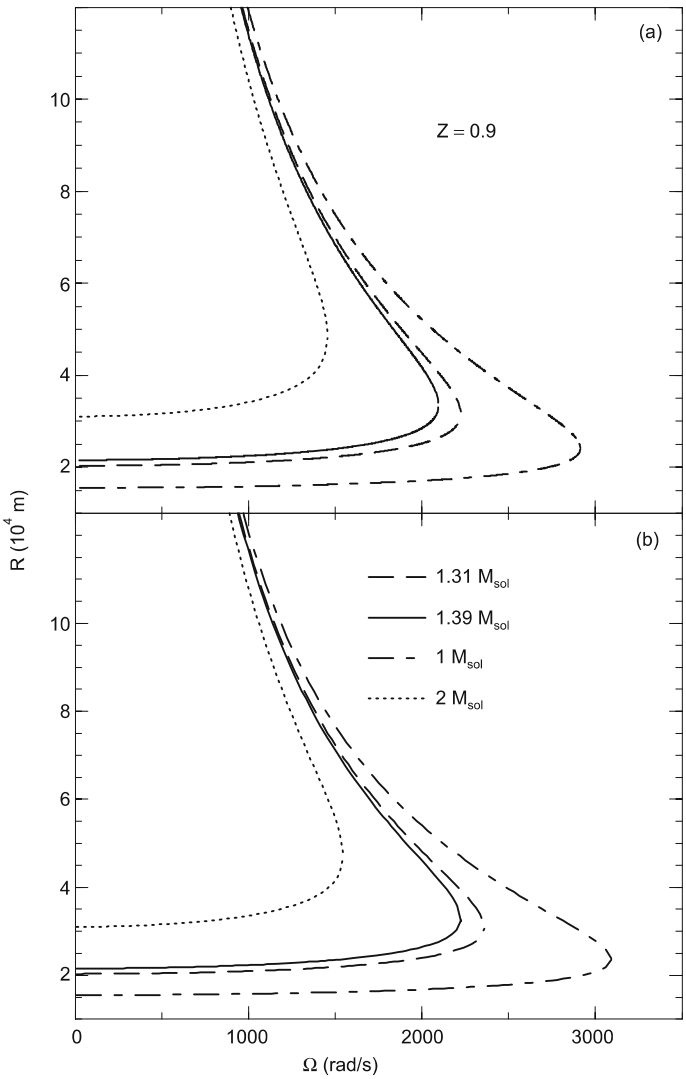

Figure 2. In these figures we show the behaviour of the two solutions r_1 and r_2 as a function of the angular velocity for different masses. The top figure **(a)** corresponds to the numerical solutions using the extended metric (33), while the bottom figure **(b)** corresponds to the analytical solutions (17, 18). Note how the solutions meet at a particular angular velocity for each mass.

In Fig. 2(b), we have plotted r_1 and r_2 *versus* the angular velocity Ω. The upper branch of each curve corresponds to the bigger radius meeting the lower value at some Ω (this will be discussed in the next section in more detail). With growing Ω the difference Δr between the two solutions becomes smaller, however, at relative small angular velocity we can opt safely for the lower value of the obtained radius (close to the Schwarzschild radius) as this is favoured by models. Such a point of view is not possible anymore with increasing Ω. Note also that the solutions $r_{1,2}$ do not determine a 'range' for the radius in the strict sense. However, since both solutions depend on the

mass, a range in the mass will determine a range for each of the two solutions. With this in mind, we can define a narrow range for the radius which will be explained below.

A plausible range for the mass can be given by the close extremes in the Gaussian distribution (2) as discussed in the introduction. For every limiting mass we will get a curve like in Fig. 2, say C_1 for the lower mass and C_2 for the upper value. The curves with an in-between mass will fill the space between the curves C_1 and C_2. A vertical tangent to the cusp[5] or maximal angular velocity of C_1 will intersect the curve C_2 in two points, r_{01} and r_{02}, which we can take as a definition of range of allowed radii. The result is a single narrow range which becomes smaller with increasing angular velocity and is zero at a maximum Ω. For instance, in the case of the neutron star PSR B1937+21, $r_{01} = 17{,}600\,\mathrm{m}$ and $r_{02} = 25{,}800\,\mathrm{m}$ such that $\Delta r = 8200\,\mathrm{m}$. The existence of the maximum angular velocity corresponding to the cusp of every curve allows even to sharpen this concept to be discussed in the next section.

It is of some interest to expand these solutions (r_1 and r_2) neglecting small terms[6] in $\mathcal{A}$ and χ. The relevant quantities can now be approximated as:

$$\Delta \approx \frac{8GM}{15c^2}, \qquad \mathcal{A} = \frac{2c}{\Omega}\sqrt{\frac{1-\mathcal{Z}^2}{3}} \tag{21}$$

and

$$\chi \approx \frac{3\sqrt{3}GM\Omega}{c^3(1-\mathcal{Z}^2)^{3/2}} + \frac{4\sqrt{3}GM\Omega}{5c^3\sqrt{1-\mathcal{Z}^2}}. \tag{22}$$

When $\chi \sim 0$, one can express r_1 and r_2 as:

$$r_1 \approx -\Delta - \mathcal{A}\left(\frac{\sqrt{3}}{2} - \frac{\chi}{6} - \frac{\chi^2}{12\sqrt{3}}\right), \tag{23}$$

$$r_2 \approx -\Delta + \mathcal{A}\left(\frac{\chi}{3} + \frac{4\chi^3}{81}\right). \tag{24}$$

The final results of our approximation reads:

$$r_1 \approx \frac{c}{\Omega}\sqrt{1-\mathcal{Z}^2} - \frac{GM}{c^2(1-\mathcal{Z}^2)} - \frac{12GM}{15c^2} - \frac{G^2M^2\Omega(4\mathcal{Z}^2-19)^2}{150c^5(1-\mathcal{Z}^2)^{5/2}}, \tag{25}$$

$$r_2 \approx \frac{2GM}{c^2(1-\mathcal{Z}^2)} + \frac{8G^3M^3\Omega^2(19-4\mathcal{Z}^2)^3}{3375c^8(1-\mathcal{Z}^2)^4}. \tag{26}$$

Note that the first term in r_2 is the Schwarzschild radius modified by a factor of $1/c^2(1-\mathcal{Z}^2)$. Actually, this term is the same result one would obtain by using a spherically symmetric metric with no rotation.

It is important to remember that this approximation starts to fail when $\chi \to 1$, which occurs at $\mathcal{Z} \to 0$.

[5] We use the word 'cusp' freely for the point where r_1 meets r_2. This should not be confused with a cusp definition in catastrophe theory, see Kusmartsev *et al.* (1991).

[6] Terms of order $(GM\Omega/c^3)^2$ and $(GM\Omega/c^3)^3$.

4. The limiting angular velocity

To understand the origin of a maximal angular velocity it is instructive to look at the generic behaviour of the function f. As already briefly mentioned, the latter will have two zeros on the positive axis and a local maximum between them. Obviously, the case where the local maximum falls below zero is a limiting case corresponding mathematically to $D = 0$ or alternatively to $r_1 = r_2$ (or in a yet different method setting $\chi = 1$ (equation 20) and physically corresponding to a maximally allowed angular velocity). The maximal angular velocities of the curves in Fig. 2(a and b) display this behaviour. After some algebra one obtains:

$$\Omega'_{\max}(\mathcal{Z}) = \frac{c^3}{32GM}\sqrt{\frac{5}{2}}\{-675 - 360(1-\mathcal{Z}^2) + 16(1-\mathcal{Z}^2)^2 + ((5+4(1-\mathcal{Z}^2))(45+4(1-\mathcal{Z}^2))^3)^{1/2}\}^{1/2}. \quad (27)$$

As described above, we can obtain the 'absolute' value of $\Omega_{\max}$ by setting $\mathcal{Z} = 0$. This is the 'absolute' upper bound on the angular velocity which turns out to be:

$$\Omega'^{(1)}_{\max} = \frac{5c^3}{32GM}. \quad (28)$$

It is comforting to compare this 'absolute' upper bound with numerical results obtained by Salgado *et al.* (1994a, 1994b). Their final empirical results depend on the maximal allowable mass and minumum stable radius for a set of realistic equations of state of neutron stars. They obtain:

$$\Omega^{(1)}_{\max} = 0.673\left(\frac{GM_s}{R_s^3}\right)^{1/2} s^{-1}, \quad (29)$$

where M_S and R_s correspond to the mass and radius of the static configuration with maximum allowable mass. When the Schwarzschild radius is set as the their minimum radius, our rough estimate has the same order of magnitude and differs by only $\sim 50\%$.

A more realistic prediction for the maximal angular velocity when $\mathcal{Z}$ is different from zero, $\Omega_{\max}$ is consistent with the largest angular velocities observed in millisecond pulsars.[7] The result for typical redshifts around $\mathcal{Z} \sim 1$ is:

$$\Omega'_{\max}(\mathcal{Z}) \approx \frac{c^3}{GM}\left(\frac{2}{3}(1-\mathcal{Z})\right)^{3/2}. \quad (30)$$

One can interpret the equation (30) in two different, but related ways. Both ways have to do with the evidence that millisecond pulsars are orthogonal rotators ($\theta = \pi/2$) (Kuzmin & Wu 1992; Backer 1998; Chen *et al.* 1998). Since the right hand side of equation (30) agrees already with the angular velocity of fast spinning objects, the emission angle θ must be close to $\pi/2$ (see equation 14). As we shall see below, this result can in turn be used to learn about the orientation of the magnetic axis in rapidly rotating objects, particularly neutron stars.

The standard model for the pulsar emission mechanism was developed independently by Pacini (1968) and Gold (1969) (see also 'lighthouse' model, Lorimer 2001),

[7] The highest observed spin rate is 716 Hz (Hessels *et al.* 2006), $\mathcal{T} = 1.5 \times 10^{-3}$ s.

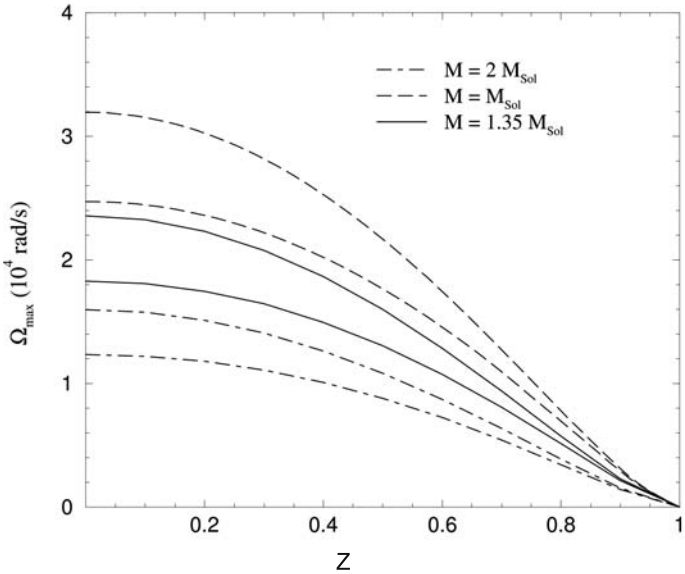

Figure 3. Maximum angular velocity as a function of the redshift for different masses. For each mass, there are two curves. The upper curve is the maximum angular velocity (equation 27) obtained from the perturbative metric. The lower curve for each mass corresponds to the analogous expression for the extended metric (33).

and will now be described briefly. Since the rotation axis is not aligned with the magnetic axis, a changing magnetic field will induce electric fields at the magnetic poles in for example, a neutron star. These electric fields will eject particles which will follow helicoidal paths around the magnetic field lines. The ejected particles will in turn, emit a narrow cone ($\sim 10^{\circ}$, Shapiro & Teukolsky 1983) of radiation parallel to the magnetic axis. From this argument it can be inferred that the angle between the magnetic axis and the rotation axis is approximately the same as the emission angle θ.

The emission angle has been measured indirectly for many pulsars by Kuzmin & Wu (1992), and in their results, a strong correlation between orthogonal magnetic axes and fast millisecond pulsars is evident. This measured correlation agrees with our results and the results of Chen *et al.* (1998) and Backer (1998), which favour orthogonal rotators.

On the other hand, we can assume the theory outlined above to be valid, which allows us to determine $\Omega_{\max}$. Indeed, we can even assume that the angular velocity of fast rotating objects is close to the maximally allowed value. In other words, we have $\Omega \approx \Omega_{\max}$ which essentially, knowing Ω, predicts the redshift. In turn, we can now extract the value of the radius. We will discuss this procedure taking realistic examples in the next section. Some examples of the behaviour of $\Omega'_{\max}$ as a function of the gravitational redshift are shown in Fig. 3.

There has been a considerable amount of work done related to the maximum angular velocity. Glendenning (1992), Koranda *et al.* (1997) and Haensel *et al.* (1999) have used empirical formulae together with extensive numerical calculations to provide a lower bound for the period of rotation. Haensel *et al.* (1999) found the minimum period

to be $T_{\min} = 0.288$ ms, assuming a mass of $1.44\,\mathrm{M}_{\odot}$. This period also depends on the minimum bound for the redshift which was found to be $\mathcal{Z} = 0.528$ (Haensel *et al.* 1999). If we use equation (27) (in accordance with the evidence of millisecond pulsars being orthogonal rotators we use $\theta = \pi/2$) and the parameters just mentioned we obtain $T_{\min} = 0.442$ ms. However, if we use our absolute bound (equation 28) and the mass assumed by Haensel, we obtain the very close value of $T_{\min} = 0.284$ ms. This is just a difference of just 1.4% which is rather gratifying recalling that our result has been obtained analytically by methods different from Haensel *et al.* (1999).

Other relevant work has been done related to the 'mass-shedding limit'.[8] This limit is conceptually different from what we have found and corresponds to the limit at which the neutron star would break apart. Lattimer and Prakash find for this limit:

$$\Omega^{(3)}_{\max}(R) = 1045\,(M/\mathrm{M}_{\odot})^{1/2}(10\,\mathrm{km}/R)^{2/3}\,\mathrm{Hz}, \tag{31}$$

which is independent of the equation of state (Lattimer & Prakash 2004) and applicable for masses not very close the maximum mass. Equation (31) can be used, for example, to find a limiting radius having an assumed or measured mass. While applying our results to find a radius we will compare our findings to the results when our maximal angular velocity is replaced by the one above. Here we note that it is not straightforward to compare the radius independent limit (equation 28) with equation (31) as the latter depends explicitly on R. However, it is obvious that both are of the same order of magnitude.

The orders of magnitude reached by the maximum angular velocity are quite large, but still less than the condition for slow rotation given by Zeldovich & Novikov (1971); even for the absolute maximum (equation 28). The condition for slow rotation ($J \ll MR_g c$) gives:

$$\Omega \ll \Omega^{(4)}_{\max} \equiv \frac{5GM}{R^2 c}, \tag{32}$$

which is one order of magnitude larger than our maximum upper bound when we take $R = R_g$, and even larger when we compare with the non-zero redshift case. Still, because our maximum angular velocity is comparable to the Zeldovich–Novikov condition, especially with $R > R_g$, we will make a better approximation for the metric in the following section.

5. Improvements: Extended metric

Even though the perturbative metric (10) gives relevant results, a better approximation for the metric is given for instance in Butterworth & Ipser (1976). Assuming a negligible quadrupole moment, the second approximation for the metric is:

$$g_{tt} = -\left\{1 - \frac{2GM}{c^2 R} - \frac{1}{6}\left(\frac{GM}{c^2 R}\right)^3 - \mathcal{O}\left[\frac{GM}{c^2 R}\right]^4\right\},$$

$$g_{t\phi} = \frac{J\sin^2\theta}{c^2 M}\left\{\frac{2GM}{c^2 R} + 4\left(\frac{GM}{c^2 R}\right)^2 + \left(\frac{GM}{c^2 R}\right)^3 + \mathcal{O}\left[\frac{GM}{c^2 R}\right]^4\right\},$$

[8] See Friedman *et al.* (1986); Lattimer *et al.* (1990); Haensel *et al.* (1995).

$$g_{\phi\phi} = \frac{R^2 \sin^2(\theta)}{c^2}\left\{1 + \frac{2GM}{c^2 R} + \frac{1}{2}\left(\frac{GM}{c^2 R}\right)^2 + \mathcal{O}\left[\frac{GM}{c^2 R}\right]^3\right\}. \tag{33}$$

One can apply the very same procedure as before. The resulting polynomial to be solved to obtain the two solutions for the radius is of fifth order in R. In consequence we can present the solution only numerically. An inspection of Figs. 2 and 3 shown that the new results, differ from the previous one only at very high angular velocities. The maximum angular velocity obtained using the extended metric is slightly higher than the one obtained analytically, so that equation (27) for the maximum angular velocity is still a valid bound. A possible quadrupole moment contribution can have the same order of magnitude as the new terms introduced here. Therefore, we would expect their impact on the results to be similar as of the improved metric elements.

6. Applications

Here, we shall apply our results to some known compact objects such as Sirius B, an isolated neutron star, and several known pulsars.

Sirius B is the binary companion of the very bright Sirius A and is the closest White Dwarf to Earth. Sirius B has been studied extensively, and the gravitational redshift has been measured accurately with the help of the Hubble space telescope (Barstow *et al.* 2005). Also, since it is a binary system, its mass has been measured accurately (Holberg *et al.* 1998).

$$\mathcal{Z} = 0.999735 \pm 0.000015; \qquad M = 0.984\,\mathrm{M}_\odot. \tag{34}$$

According to equation (27), we get a minimum period of

$$\frac{\mathcal{T}_{\min}(\text{Sirius B})}{\sin\theta} = 10.8\,\text{s}. \tag{35}$$

This number does not change very much, had we applied the results from the extended metric.

The low mass X-ray binary system EXO 0748-676 has been studied by Cottam *et al.* (2002). They managed to measure spectral absorption lines corresponding to a redshift of

$$\mathcal{Z} = 0.74. \tag{36}$$

This together with its mass (assumed to be $1.35\,\mathrm{M}_\odot$) gives:

$$\mathcal{T}_{\min}(\text{EXO 0748-676}) = 9.05 \times 10^{-4}\,\text{s}. \tag{37}$$

The value above has been obtained by employing the extended metric (the corresponding value resulting from the first order approximation is 5.8×10^{-4} s). The period for this neutron star has been measured to be 22×10^{-3} s (Villarreal & Strohmayer 2004), which is not too far away from the above limit given by $\mathcal{T}_{\min}$. The predicted radius for the assumed mass and measured period and redshift, is 8.7 km.

In addition to the previous applications, our results concerning the maximum angular velocity, can be applied to millisecond pulsars. It is plausible to assume that for

Table 1. Predicted maximum $\mathcal{Z}$ and maximum radius for several pulsars assuming that they are rotating at their maximum angular velocity. We also assumed these pulsars are orthogonal rotators. For the case of PSR B1937+21, 1855 + 09 and 0531 + 21, θ was measured to be 90° by Kuzmin & Wu (1992). Note that the last three maximum radii are noticeably larger than what is generally predicted using equations of state for nuclear matter. The lack of accuracy shows the limitations of our formalism when the redshift is not known, and is most likely due to the violation of our maximum angular velocity assumption. The low angular velocity is especially noticeable when compared with the absolute maximum angular velocity (equation 28).

Pulsar	Period (ms)	M ($M_\odot$)	$\mathcal{Z}$	R (km)
PSR J1748-2446ad (Hessels *et al.* 2006)	1.396	1.35?	0.834	≤ 20.1
PSR B1937+21 (Ashworth *et al.* 1983)	1.557	1.35?	0.836	≤ 20.2
PSR J1909-3744 (Jacoby *et al.* 2003)	2.95	1.438	0.896	≤ 31.1
PSR 1855+09	5.3	1.35?	0.935	≤ 46.9
PSR J0737-3039 A (Lyne *et al.* 2004)	22.7	1.34	0.976	≤ 133.6
PSR 0531+21	33.3	1.35?	0.982	≤ 164.4
PSR B1534+12 (Stairs *et al.* 1998)	37.9	1.34	0.983	≤ 165.9

millisecond pulsars, the measured angular velocity is very close to the maximum angular velocity. With this in mind, it is possible to predict a value for $\mathcal{Z}$ using equation (30), and a unique value for the radius using equation (17) or (18). Since $\Omega_{\max}(\mathcal{Z})$ is a decreasing function, the predicted $\mathcal{Z}$ is actually a maximum bound, and if the 'preferred' radius for the neutron star is r_2, the predicted radius can be thought of as a maximum bound also. Here we present a table with predicted redshifts and radii for several fast millisecond pulsars.

From the table it can be inferred that for fast millisecond pulsars the radii are consistent with standard neutron star models (Shapiro & Teukolsky 1983). However, for the slower millisecond pulsars, the maximum radius is slightly greater than what is predicted by most neutron star models, which implies that these neutron stars are probably not rotating exactly at their maximum angular velocity. In such a case the given radii should be interpreted as an upper bound which comes indeed close to the upper limit discussed in the introduction. Using equation (31) and assuming a mass of 1.4 $M_\odot$, the corresponding radius for PSR B1937+21 turns out to be 15.5 km (Lattimer & Prakash 2004), 5 km less than our result. For the slower millisecond pulsars, our results also predict slightly larger radii than those obtained by equation (31).

7. Conclusions

To summarize our main findings we mention the derivation of the maximal angular velocities, one which is dependent of the gravitional redshift (equation 27) and the other one which sets an absolute limit depending only on the mass (equation 28).

The maximal angular velocity derived in text does not depend on the radius directly, but on the redshift which makes direct contact with existing or future observations. The absolute limit on Ω (equation 28) does not even depend on the redshift and it is worth pointing out that its order of magnitude is comparable to the results obatined elsewhere. It is satisfying that both these bounds come close to the observed values for millisecond pulsars. This implies that nature reaches here its maximally possible value. Another advantage of our approach is the confirmation of the emission angle of radiation in fast rotating neutron stars. The application of our results to existing objects clearly show that the method of using the gravitational redshift for rotating objects is effective.

Secondly, we have shown that the gravitational redshift in conjunction with global results from theoretical models can yield valuable information on the properties of rotating compact objects.[9] Even though the determination of the radius in the presence of rotation is not a unique prescription, for relatively small angular velocities we can always opt for the lower result of the radius determination. With increasing angular velocity, a narrow range of possible radii can be defined. Alternatively, assuming that the angular velocity of the fast spinning neutron stars is close to its maximal value, we can either obtain a unique radius or an upper bound.

The important feature we would like to emphasize here is that we relate properties of rotating compact objects to measurable quantities such as the gravitational redshift and the angular velocity. This way, our approach is semi-empirical and independent of model details.

As discussed in section four, our analytical findings regarding the maximal angular velocity agree with results obtained after numerical calculations. In this way, both, the analytical and numerical approach, corroborate each other.

Acknowledgement

We would like to thank Paolo Gondolo, University of Utah, for useful discussions and carefully reading the manuscript.

References

Ashworth, M., Lyne, A. G., Smith, 1983, *Nature*, **301**, 313.
Baade, W., Zwicky, F. 1934, *Phys. Rev.*, **45**, 138.
Backer, D. C. 1998, *ApJ*, **493**, 873–878.
Barstow, M. A., Burleigh, M. R., Holberg, J. B., Hubeny, I., Bond, H. E., Koester, D. 2005, 4th European Workshop on White Dwarfs, *ASP Conf. Ser.*, 334.
Baym, G., Lamb, F. K. 2005, *Encyclopedia of Physics*, 1721–1725.
Becker, W., Pavlov, G. 2002, astro-ph/0208356.
Bronstein, I. N., Semendjajew, K. A. 2004, *Handbook of Mathematics*, Springer, Berlin.
Butterworth, E. M., Ipser, J. R. 1976, *ApJ*, **204**, 200–223.
Carroll, S. M. 2004, Spacetime and Geometry, Pearson Addison Wesley.
Chen, K., Ruderman, M., Zhu, T. 1998, *ApJ*, **493**, 397–403.
Cook, G. B., Shapiro, S. L., Teukolsky, S. 1994, *ApJ*, **424**, 823–845.
Cottam, J., Paerels, F., Mendez, M. 2002, *Nature*, **420**, 5154.

[9] It is fair to say in this context that as for now there are not many reliable measurements of the gravitational redshift.

Friedman, J. L. 1995, Milisecond Pulsars: A decade of surprise, *ASP Conf. Ser.* (eds) Fruchter, A. S., Tavani, M., Becker, D. C., **72**, 177.
Friedman, J. L., Parker, L., Ipser, J. R. 1986, *ApJ* **304**, 115.
Glendenning, N. K. 1992, *Phys. Rev. D*, **46**, 4161.
Gold, T. 1969, *Nature*, **221**, 25–27.
Haensel, P., Lasota, J. P., Zdunik, J. L. 1999, *Astron. Astrophys.*, **344**, 151–153.
Haensel, P., Salgado, M., Bonazzola, S. 1995, *Astron. Astrophys.*, **296**, 745.
Hessels, J. W. T., Ransom, S. M., Stairs, I. H., Freire, P. C. C., Kaspi, V. M., Camilo, F. 2006, *Science*, **311**, 1901–1904.
Holberg, J. B., Barstow, M. A., Bruhweiler, F. C. 1998, *ApJ*, **497**, 935–942.
Jacoby, B. A., Bailes, M., van Kerkwijk, M. H., Ord, S., Hotan, A., Kulkarni, S. R., Anderson, S. B. 2003, *ApJ*, **599**, L99–L102.
Koranda, S., Stergiulas, N., Friedman, J. L. 1997, *ApJ*, **488**, 799.
Krisher, T. P., Morabito, D., Anderson, J. D. 1993, *Phys. Rev. Lett.*, **70**, 2213.
Kusmartsev, F. V. *et al.*, 1991, *Phys. Lett.*, **A157**, 465.
Kuzmin, A. D., Xinji, Wu 1992, *Astrophys. Space Sci.*, **190**, 209–218.
Lattimer, J. M., Prakash, M. 2004, *Science*, **304**, 536–542.
Lattimer, J. M., Prakash, M., Masak, D., Yahil, A. 1990, *ApJ*, **304**, 241.
Lorimer, D. R. 2001, *Living. Rev. Relativity*, **4**, 5.
Luminet, J. P. 1979, *Astron. Astrophys.*, **75**, 228.
Lyne, A. G., Burgay, M., Kramer, M. 2004, *Science*, **303**, 1153.
Manko, V. S., Mielke, E. W., Sanabria-Gomez, J. D. 2000, *Phys. Rev. D*, **61**, 081501.
Mielke, E. W. 2001, *Phys. Rev. D*, **63**, 044018.
Oppenheimer, J. R., Volkov, G. M. 1939, *Phys. Rev.*, **55**, 374.
Pachon, L. A., Rueda, J. A., Sanabria-Gomez, J. D. 2006, *Phys. Rev. D*, **73**, 104038.
Pavlov, G., Zavlin, V. E. 2003, In: *Proceedings 21st Texas Symposium on Relativistic Astrophysics* (eds) Bandiera, R., Maiolino, R., Mannucci F., World Scientific, arXiv:astro-ph/0305435.
Pacini, F. 1968, *Nature*, **219**, 145–146.
Rhoades, C. E., Ruffini, R. 1974, *Phys. Rev. Lett.*, **32**, 324.
Salgado, M., Bonazzola, S., Gourgoulhon, E., Haensel, P. 1994a, *Astron. Astrophys.*, **291**, 155.
Salgado, M., Bonazzola, S., Gourgoulhon, E., Haensel, P. 1994b, *Astron. Astrophys. Suppl.*, **108**, 455.
Schunck, F. E., Mielke, E. W. 2003, *Class. Quant. Grav.*, **20**, R301.
Shapiro, S. L., Teukolsky, S. A. 1983, *The Physics of Compact Objects*, John Wiley & Sons.
Snider, J. L. 1972, *Phys. Rev. Lett.*, **28**, 853.
Stergioulas, N. 2003, *Living. Rev. Relativity*, **6**, p. 3.
Stairs, I. H., Arzoumanian, Z., Camilo, Z., Lyne, A. G., Nice, D. J., Taylor, J. H., Thorsett, S. E., Wolszczan, A. 1998, *ApJ*, **505**, 352.
Thorsett, S. E., Chakrabarty, D. 1999, *ApJ*, **512**, 288, astro-ph/9803260.
Vadya, P. C. 1951, *Proc. Indian. Acad. Sci.*, **A33**, 264.
Villarreal, A. R., Strohmayer, T. E. 2004, *ApJ*, **614**, L121.
Wald, R. W. 1984, *General Relativity*, University of Chicago Press.
Zeldovich, Y. B., Novikov, I. D. 1971, *Stars and Relativity*, Dover.